International Journal of Thermal Sciences 118 (2017) 386–396

Contents lists available at ScienceDirect

International Journal of Thermal Sciences

journal homepage: www.elsevier.com/locate/ijts

Numerical solution of three-dimensional N-S equations and energy in the case of unsteady stagnation-point flow on a rotating vertical cylinder

Reza Bayat Ph.D Student [a], Asghar B. Rahimi Professor [b, *]

[a] Mechanical Engineering, P.O. Box No. 91775-1111, Mashhad, Iran
[b] Faculty of Engineering, Ferdowsi University of Mashhad, P.O. Box No. 91775-1111, Mashhad, Iran

ARTICLE INFO

Article history:
Received 13 February 2017
Received in revised form
7 April 2017
Accepted 10 May 2017

Keywords:
Numerical solution
Three-dimensional navier-stokes equations
Stagnation-point flow
Rotating vertical circular cylinder
Mixed convection

ABSTRACT

The three-dimensional unsteady problem of impulsive stagnation-point flow on a rotating vertical circular cylinder along with mixed convection heat transfer has been solved, numerically for the first time. This is because similarity solution techniques are not always possible to be accomplished. Initially, the fluid is considered to be at rest and with a uniform temperature T_∞ and at $t = 0$ it starts flowing toward a vertical cylinder at the strength rate of $\bar{k}$ and the cylinder surface's temperature rises to T_w, simultaneously. The cylinder possesses a rotational movement, with a constant angular velocity ω. The Navier-Stokes and energy equations in cylindrical coordinate system have been descritized and solved in a 2-D domain by using a SIMPLE based algorithm. The buoyancy effects are also included in the computations, so the problem is investigated as mixed convection heat transfer. Considering a sample case of incompressible flow with $Re = 1,5,10,15,20$ and $\mathrm{Pr} = 0.7$, the results of Nusselt number, wall shear-stress and dimensionless velocity and temperature have been obtained at different states of cylinder's wall temperature and for some selected values of Grashof numbers.

1. Introduction

The problem of stagnation-point flow and heat transfer on a plate or cylinder has always been a high interested issue to study because of its various industrial applications. For example, in manufacturing of metal, plastic or food products by extrusion process, the output product is usually cooled by blowing a peripheral fluid flow. Since the cooling process affects the resistance and quality of the product, analytical modeling and evaluation of this physical event is investigated under the topic of stagnation-point flow problem. Some more applications such as paint spraying and de-icing can be mentioned here. By using analytical methods, particularly similarity solutions, accurate results can be obtained demonstrating flow behavior in viscous boundary layer. However, finding the appropriate similarity variables and solving the governing differential equations of the problem are the main challenges of this kind of approaches. Besides, the solvable self-similar or semi-similar equations can be produced for only few specific boundary conditions. The history of the analytical methods studies using similarity solution techniques goes back to Hiemenz [1]. He investigated the steady two-dimensional laminar incompressible flow perpendicularly impinging on a flat plate and succeeded to transform governing equations into ordinary differential equations which then were solved by using numerical methods. Wang [2] was the first who presented the solution of stagnation-point flow on a circular cylinder. This problem was for the simple case of a stationary cylinder without suction and blowing in steady-state condition and its importance was due to introducing different similarity variables for cylindrical coordinate system. Based on Wang's accomplishment, Gorla [3] could obtain both velocity and temperature distributions for a cylinder with constant wall temperature and constant heat flux. He considered energy equation and used a transformation for temperature quantity, then solved the extracted differential equations by numerical methods. Gorla [4,5] continued his work and solved the problem for transient state when the free stream flow has time-dependent velocity. He used series form solution in his analysis and presented the results for some specific time-dependent functions. Also, Gorla [6] considered viscous dissipation effects in the equation of heat transfer and presented the numerical results for this case. Gorla [7] also

* Corresponding author.
E-mail address: rahimiab@um.ac.ir (A.B. Rahimi).

http://dx.doi.org/10.1016/j.ijthermalsci.2017.05.007
1290-0729/

Nomenclature

a	cylinder radius
b	constant coefficient
f	dimensionless velocity function
g	gravitational acceleration
Gr	Grashof number
h	convective heat transfer coefficient
i,j	indexes of a point in r-z grid
k	thermal conductivity
$\overline{k}$	strength of the free stream flow
n	index of time level
Nu	Nusselt number
p	dynamic pressure
pr	Prandtl number
r	dimensionless co-ordinate in radial direction of cylinder
R_{max}	Position of the solution domain's boundary in r-direction
Re	Reynolds number
t	time
T	temperature
T_w	temperature on the cylinder's wall
T_∞	free stream temperature
u, v, w	dimensionless viscous flow's r
φ and z	component of velocity
U, V, W	dimensionless invicsid flow's r
φ and z	component of velocity
z	dimensionless co-ordinate in axial direction of cylinder
z_s	position of stagnation-point on the cylinder's surface along z-axis
Z_{max}	Upper limit of the solution domain's boundary in z-direction
Z_{min}	Lower limit of the solution domain's boundary in z-direction
α	thermal diffusivity
β	volumetric thermal expansion coefficient
θ	dimensionless temperature
μ	dynamic viscosity
ν	kinematics viscosity
ρ	density
τ	dimensionless time
τ_w	dimensionless shear stress on the cylinder's wall
φ	angular coordinate
ω	angular velocity of cylinder
Ω	dimensionless rotation rate, $\omega/\overline{k}$

presented a non-similar situation by supposing a cylinder with axial movement which is proportional to the axial velocity of the free stream flow. He obtained the velocity distributions for various positive and negative velocities of the cylinder's wall. Gorla [8,9,and10] in his next papers assumed the cylinder having harmonic motion and obtained the results of this unsteady problem for two cases of low and high frequencies. He also studied convection of a vertical circular cylinder impinged by a normal stagnation-point flow and presented numerical solution of the equations in the case of constant or linearly variable wall temperature in Refs. [11,12]. Cunning et al. [13] in his paper dealt with solving the problem of normal stagnation-point flow on a rotating cylinder with uniform transpiration which is actually with a different boundary conditions comparing to past Gorla's studies. Takhar et al. [14] investigated the unsteady case of this problem for any arbitrary time-dependent free-stream or cylinder velocities. They obtained numerical methods for solving their final differential equations for the cases of semi-similar and self-similar forms. Gorla et al. [15] used Chebyshev approximation to solve the heat transfer equation in the axisymmetric stagnation-point flow on a cylinder which is only a different analytical approximation method to obtain temperature distribution. Rahimi [16] presented a perturbation solution for the problem of heat transfer in an axisymmetric stagnation-point flow at high Reynolds numbers by using an inner and outer expansions. Saleh and Rahimi [17,18] in two papers presented the similarity solution of axisymmetric stagnation-point flow and heat transfer on a moving cylinder when it has time-dependent axial velocity and uniform transpiration with selected examples of this movement. Rahimi [19] and Saleh [20] in two separate papers expressed a solution by perturbation techniques for stagnation-point flow and heat transfer on a moving cylinder with transpiration when Reynolds number was high, which is again usage of an inner and outer expansion in obtaining a uniformly valid solution for temperature distribution. Saleh and Rahimi [21] considered constant rotational velocity and time-dependent angular velocity for a cylinder in axisymmetric radial stagnation-point flow. They used similarity solution to solve this problem, too and for selected examples for the angular rotation of the cylinder. Wang [22] replaced partial slip condition instead of no-slip condition on the wall for the basic problem of stagnation-point flow on an axially moving cylinder and solved it by similarity solution which is again the same kind of solutions and only for different boundary conditions. Rahimi and Saleh [23] dealt with the same problem by considering rotational movement for the cylinder with time-dependent angular velocity. Also, they [24] solved the problem of axisymmetric stagnation-point flow and heat transfer on the cylinder when it has simultaneous axial and rotational movement along with transpiration which is actually a superposition of the two previously obtained solutions. Rahimi and Saleh [25] investigated the problem of unaxisymmetric heat transfer in stagnation-point flow on a cylinder with simultaneous axial and rotational movements which is caused by unaxisymmetric distribution of wall temperature or wall heat flux around the cylinder's surface which can bring in much more results depending on the different forms of this distribution. Revnic et al. [26] dealt with mixed convection heat transfer problem of a circular cylinder impinged by a normal stagnation-point flow which was already mentioned by Gorla [11] and presented its numerical solution for a wider range of dimensionless numbers. Haghighi and Rahimi [27] supposed time-dependent transpiration, axial and rotational movements for a cylinder to present a similarity solution for the case of axisymmetric stagnation-point flow and heat transfer which adds to more examples of semi-similar existing solutions. Lok et al. [28] added the stretching or shrinking effects to the problem of mixed convection heat transfer of the axisymmetric stagnation-point flow on a cylinder, which was already solved by Gorla [11]. Mohammadiun et al. [29,30] were the first who introduced the similarity variables for solving stagnation-point flow and heat transfer of a compressible fluid on a stationary cylinder. They could include the effect of variable density in the resulting similar forms of velocity and temperature equations, which should have been solved simultaneously. Najib et al. [31,32] in their two papers dealt with stagnation-point flow and heat transfer on a stretching/shrinking cylinder with surface permeation. Alizadeh et al. [33]

investigated the unaxisymmetric stagnation-point flow and heat transfer on a moving cylinder with time-dependent axial velocity and non-uniform normal transpiration which allows for all kinds of examples of non-symmetric flow by use of again similarity solution methods. Rahimi et al. [34] solved their previous compressible fluid problem with an axially moving cylinder which is use of similarity solutions with different kinds of boundary conditions.

In all the above works, the similarity solution techniques were used. Although this method of solution has high importance from mathematical point of view, it has limitations too especially when we encounter various physical conditions such as time-dependent states. That's why in the present analysis and for the first time, we solve the unsteady problem of mixed convection heat transfer from a vertical circular cylinder impinged by an impulsive axisymmetric stagnation-point flow by employing numerical methods. By applying an implicit numerical solution to three-dimensional Navier-Stokes and energy equations in a two-dimensional zone at any φ cross-section with appropriate boundary conditions, the velocity and temperature parameters are obtained directly. It's considered that a constant-strength axisymmetric outer flow impinges on a vertical circular cylinder along with gravitational effects. The flow is considered inviscid far from the cylinder but in the region near the surface (solution domain), equations of viscous flow and energy are descritized according to the finite-difference scheme and the resulting system of equations is solved by the well-known TDMA algorithm. The results were first verified by comparing to Gorla's [3] for the specific case of $T_w = const.$, $Re = 1$, 10 and $Gr = 0$, and then more results were obtained for different values of Re and non-zero Grashof numbers, too.

2. Problem formulation

Axisymmetric incompressible stagnation-point flow impinges impulsively on a rotating vertical circular cylinder with radius a, and the length of infinity with angular velocity ω and wall temperature T_w in the space influenced by gravity acceleration g. A schematic of this problem is presented in Fig. 1.

It is obvious that for the upper half of the geometry (i.e. $z > 0$) the buoyancy forces are in the same direction with the flow and so, here we have an assisting flow condition. In the contrast, for $z < 0$ there is opposing state of flow because the fluid flows downward. If the flow far from the cylinder's surface is assumed as an inviscid flow with rate of strength $\bar{k}$, then according to the axisymmetric coordinate system (r, φ, z) in Fig. 1, by referring to Wang [2], the velocity components U and W for this free stream flow, are expressed as:

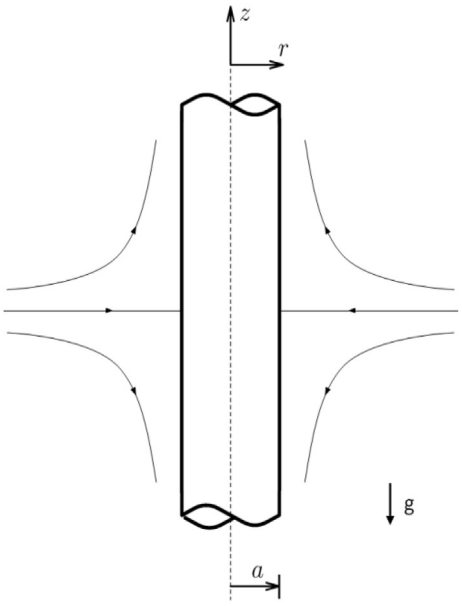

Fig. 1. Schematic of axisymmetric stagnation flow on a vertical circular cylinder.

$$\begin{cases} U = -\left(r - \dfrac{1}{r}\right) \\ W = 2z \end{cases} \tag{1}$$

In which, coordinates r and z are non-dimensionalized with the radius a, and the velocities U and W with $a\bar{k}$.

2.1. Governing equations

Supposing an incompressible viscous flow in the axisymmetric cylindrical coordinate system, the basic time-dependent equations in terms of velocity components $u\,(r, z, t)$ in r-direction, $v(r, z, t)$ in φ-direction, $w(r, z, t)$ in z-direction and temperature field $T(r, z, t)$ have the following dimensionless forms:

Mass continuity:

$$\frac{\partial}{\partial r}(ru) + r\frac{\partial w}{\partial z} = 0 \tag{2}$$

Momentum continuity (Navier-Stokes Equations):

$$2\frac{\partial u}{\partial \tau} + u\frac{\partial u}{\partial r} + w\frac{\partial u}{\partial z} = -\frac{\partial p}{\partial r} + \frac{1}{2\mathrm{Re}}\left(\frac{\partial^2 u}{\partial r^2} + \frac{1}{r}\frac{\partial u}{\partial r} - \frac{u}{r^2} + \frac{\partial^2 u}{\partial z^2}\right) \tag{3}$$

$$2\frac{\partial v}{\partial \tau} + u\frac{\partial v}{\partial r} + \frac{uv}{r} + w\frac{\partial v}{\partial z} = \frac{1}{2\mathrm{Re}}\left(\frac{\partial^2 v}{\partial r^2} + \frac{1}{r}\frac{\partial v}{\partial r} - \frac{v}{r^2} + \frac{\partial^2 v}{\partial z^2}\right) \tag{4}$$

$$2\frac{\partial w}{\partial \tau} + u\frac{\partial w}{\partial r} + w\frac{\partial w}{\partial z} = -\frac{\partial p}{\partial z} + \frac{1}{2\mathrm{Re}}\left(\frac{\partial^2 w}{\partial r^2} + \frac{1}{r}\frac{\partial w}{\partial r} + \frac{\partial^2 w}{\partial z^2}\right) + \frac{Gr}{4\mathrm{Re}^2}\theta \tag{5}$$

The velocities components u, v and w are non-dimensionalized with $a\bar{k}$ and pressure p with $\rho a^2\bar{k}^2$. Also, dimensionless time τ and temperature θ have the following expressions:

$$\tau = 2\bar{k}t,\ \theta = \frac{T - T_\infty}{T_w - T_\infty} \tag{6}$$

The last term in Eq. (5) is due to the presence of buoyancy forces in z-direction which is according to the Boussinesq's approximation.

Energy equation:

$$2\frac{\partial \theta}{\partial \tau} + u\frac{\partial \theta}{\partial r} + w\frac{\partial \theta}{\partial z} = \frac{1}{2\mathrm{Re}\cdot\mathrm{Pr}}\left(\frac{\partial^2 \theta}{\partial r^2} + \frac{1}{r}\frac{\partial \theta}{\partial r} + \frac{\partial^2 \theta}{\partial z^2}\right) \tag{7}$$

Where, the Reynolds, Prandtl and Grashof numbers have the following definitions:

$$\mathrm{Re} = \frac{\bar{k}a^2}{2\upsilon},\ \mathrm{Pr} = \frac{\upsilon}{\alpha},\ Gr = \frac{g\beta(T_w - T_\infty)a^3}{\upsilon^2} \tag{8}$$

The boundary conditions of the problem with respect to the no-slip condition and $T = T_w$ on the cylinder's surface, in one side, and inlet inviscid flow with T_∞ from another side of the domain of solution, are:

$$r = 1:\ u = w = 0,\ v = \Omega = \omega/\bar{k}\ and\ \theta = 1$$
$$r = R_{max}:\ u = U,\ v = 0,\ w = W\ and\ \theta = 0 \quad (9)$$

For outlet boundaries, which are far enough from the stagnation point, we approximate the velocity field by analytical inviscid flow relations expressed in Eq. (1) and then we will have:

$$z = Z_{min}, Z_{max}:\ \frac{\partial u}{\partial z} = 0,\ \frac{\partial w}{\partial z} = 2 \quad (10)$$

Also, we extrapolate θ by two previous points as the boundary condition of the temperature at outlets. Since unsteadiness of the problem is a consequence of impulsive motion of the free stream flow at $t = 0$, we consider the fluid at rest (no motion) with uniform temperature T_∞ in both fluid and cylinder's wall for $t < 0$ as initial conditions. A sudden free-stream flow, according to Eq. (1), appears for $t \geq 0$ in which the cylinder's wall temperature rises to T_w simultaneously.

2.2. Flow characteristics

When numerical results of the velocity and temperature field are determined, Nusselt number and wall shear-stress, which is non-dimensionalized by $\mu\bar{k}$, can be obtained from the following relations by a forward difference approximation:

$$Nu = \frac{ha}{2k} = -\frac{1}{2}\left[\frac{\partial\theta}{\partial r}\right]_{r=1},\ (\tau_w)_\varphi = \left[r\frac{\partial}{\partial r}\left(\frac{v}{r}\right)\right]_{r=1},\ (\tau_w)_z = \left[\frac{\partial w}{\partial r}\right]_{r=1} \quad (11)$$

Naturally, the position of the stagnation point on the cylinder's surface (z_s), is somewhere along the z-axis where $(\tau_w)_z = 0$.

3. Method of solution

Equations (3)–(7) under boundary conditions (9)–(10) are solved numerically using an implicit finite-difference scheme based on SIMPLE method in numerical method. For this purpose, we provide a computer code in Fortran language. Because of the problem axisymmetry, we choose a rectangular zone as a 2-D domain of solution in r-z-plane which is located between $r = 1$ to $r = R_{max}$ and $z = Z_{min}$ to $z = Z_{max}$ (Fig. 2). This domain which is typically meshed by a staggered square grid system is shown in Fig. 3. All first-order and second-order derivatives with respect to r *and* z are discretized using a central difference formulation, whereas the first-order derivatives in τ are replaced by a backward difference approximation (for example $\partial u/\partial\tau$ is approximated by $(u^{n+1}\text{-}u^n)/\Delta\tau$). Besides, the coefficient in the nonlinear convective terms is approximated by the known value from previous time level, for instance:

$$u\frac{\partial u}{\partial r} \approx u_{i,j}^n \frac{u_{i+1,j}^{n+1} - u_{i-1,j}^{n+1}}{2\Delta r},\ w\frac{\partial u}{\partial z} \approx w_{i,j}^n \frac{u_{i,j+1}^{n+1} - u_{i,j-1}^{n+1}}{2\Delta z}$$

At each time level, the procedure iterates until the results of velocity converge to the stable values with the accuracy up to sixth decimal place. The same procedure is repeated for the next time step and the problem solution continues to a value of τ where the results show steady state behavior. To investigate the independency of the grid size we employed several various step sizes. The graphical results for the distribution of axial velocity w and thermal function θ are shown in Fig. 4 for $Re = 1$, $pr = 0.7$, $Gr = 0$, $R_{max} = 4$ and $Z_{min,max} = \pm 3$. As can be seen, the profiles of the velocity and temperature distribution are so close for all the step sizes listed in Fig. 4, therefore we made a comparison between inlet and outlet

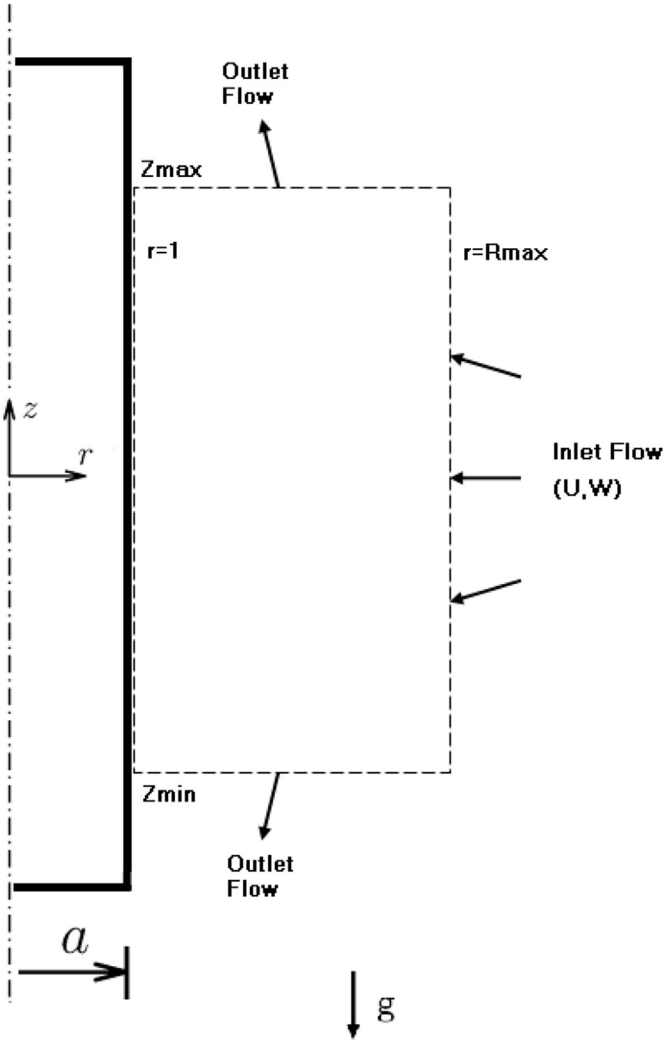

Fig. 2. Illustration of the Domain of the solution.

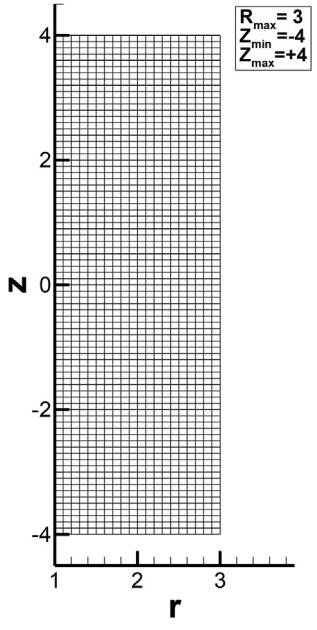

Fig. 3. Sample of the meshed domain.

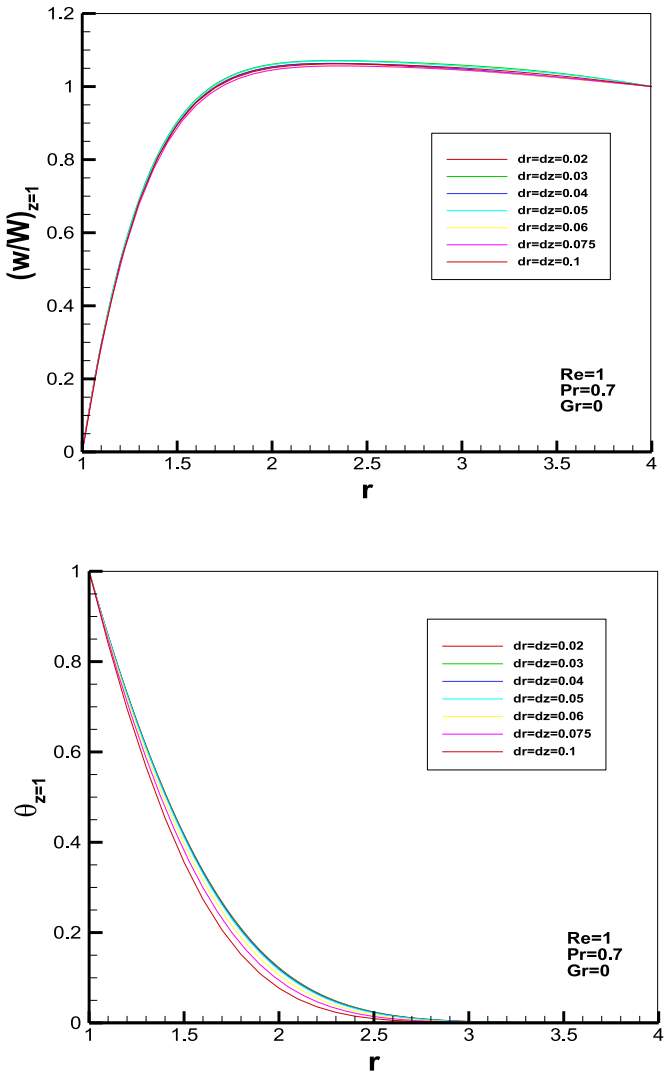

Fig. 4. Distribution of axial velocity $w\ (r, z)$ and thermal function θ at $z = 1$ for $Re = 1$, $pr = 0.7$, $Gr = 0$ and $R_{max} = 4$, $Z_{min,max} = \pm 3$.

flow rate of the solution domain tabulated in Table 1. The best choice of grid size would be $\Delta r = \Delta z = 0.05$ which leads to the minimum difference between inlet and outlet flow rate. For the values of Δr and Δz less than 0.02 because of truncation errors accumulation, no convergence with our expected accuracy would occur.

4. Results and discussions

We used the results by Gorla [3] in order to validate our computational code for the case of steady-state flow on a constant-wall-temperature cylinder. This comparison for dimensionless function f with the same parameters $Re = 1$, $Pr = 1$ and no buoyancy effects ($Gr = 0$) are shown in Fig. 5. Note that the dimensionless function f is equal to $[-ru]$ and it has been employed by Gorla in his similarity solution. Also, the comparison of dimensionless temperature θ has been shown in Fig. 6. The numerical results of the computational code in these two figures have been obtained for different values of R_{max}, whereas the values of Z_{min} and Z_{max} are fixed and equal to -3 and $+3$, respectively. It is observed that the results of the numerical solution and the similarity one are very close, especially for small r, but doesn't match exactly because we know that the similarity solution is actually a consequence of asymptotic situation $R_{max} \to \infty$. Also, by choosing greater values of R_{max}, we would not find the results necessarily closer to the similarly solution, so that the minimum difference between our results and Gorla's can be seen for $R_{max} = 6$ and$R_{max} = 8$ for two functions f and θ, respectively.

Another comparison between our numerical results and Gorla's is shown in Fig. 7 for $Re = 10$. For this value of Reynolds number, we choose $R_{max} = 2.8$ to have the best converging situation in the solution procedure. Here again, we observe that for the values of r close to the cylinder's surface, there is a good agreement between present results and Gorla's solution for the velocity function f and the thermal function θ.

Now, consider the case of the steady-state stagnation-point flow on a cylinder with constant wall temperature, $Pr = 0.7$ and no gravity $(Gr = 0)$, which is the case of pure forced convection with no free convection effect. We conducted our computations in a solution domain with various $R_{max} = 2.6, 2.8, 3,6$and $Z_{max,min} = \pm 4$ for three different Reynolds numbers. Distribution of the axial velocity (w/W) and the thermal function θ against r at the specific value of $z = 1$are shown in Figs. 8–10. Moreover, the results of the Nusselt number and the dimensionless shear-stress on the cylinder's wall, $(\tau_w)_\phi$ and $(\tau_w)_z$, are plotted in Figs. 10–12. According to Fig. 8, at higher Reynolds numbers the boundary layer contracts toward the cylinder's wall. As can be seen, for $Re = 20$ there is an intensive gradient of axial velocity (w/W) until about $r = 1.2$ which denotes the boundary layer region and for $Re = 10$ it exists until $r = 1.4$. After that, we see a smooth variation in the velocity diagram, which is

Table 1
Inlet and outlet flow rate related to the solution domain with dimensions $R_{max} = 4$ and $Z_{max,min} = \pm 3$.

Step size	Q_{in}	Q_{out}	Error (%)
$\Delta r = \Delta z = 0.02$	565.4867	563.7842	0.301068
$\Delta r = \Delta z = 0.03$	565.4867	567.4353	0.344588
$\Delta r = \Delta z = 0.04$	565.4867	563.7758	0.302554
$\Delta r = \Delta z = 0.05$	565.4867	566.2092	0.127766
$\Delta r = \Delta z = 0.06$	565.4867	563.8697	0.285948
$\Delta r = \Delta z = 0.075$	565.4867	564.1638	0.23394
$\Delta r = \Delta z = 0.1$	565.4867	564.3403	0.202728

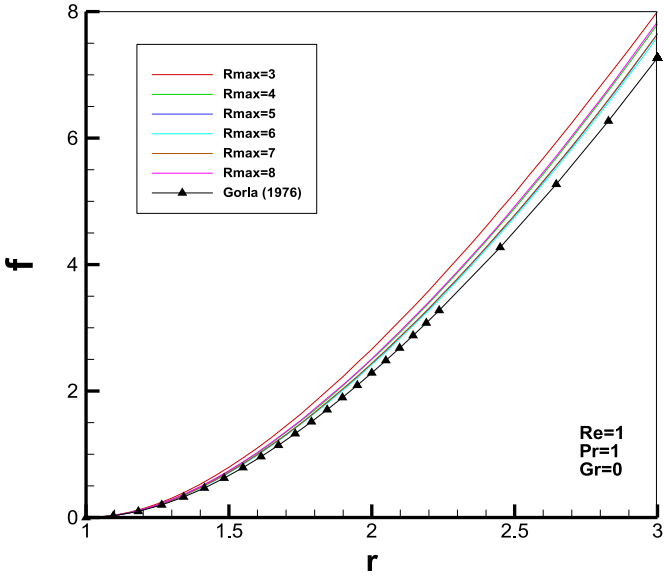

Fig. 5. Distribution of the steady state radial velocity function f at $z = 3/4$ for $Re = 1$,$Pr = 1$, $Gr = 0$ and $Z_{min,max} = \pm 4$with different values of R_{max}.

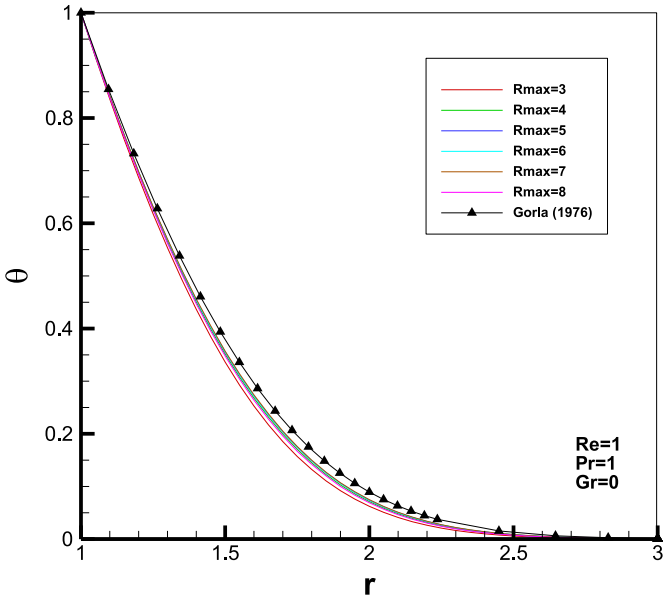

Fig. 6. Distribution of the steady-state thermal function $\theta\ (r, z = 3/4)$ for $Re = 1$,$Pr = 1$, $Gr = 0$ and $Z_{\min,\max} = \pm 4$with different values of $R_{\max}$.

related to the outside region of the boundary layer. But for $Re = 1$, these two regions are not clearly distinguishable and it is better to use a calculation domain with larger dimension $R_{\max}$ for this low Reynolds number. According to Fig. 9, one can see how a rotating cylinder causes the velocity component v in the flow field at any Reynolds number. The fluid boundary affected by this rotational movement is about $r = 2.65, 1.75, 1.55, 1.45, 1.35$ for $Re = 1, 5,10,15,20$, respectively. According to Fig. 10, the thermal boundary layer for $Re = 1, 5, 10, 15, 20$ expands to $r = 2.8, 1.8, 1.6$, 1.45, 1.4 approximately, and has very close and similar distribution to the v-component velocity. Our calculation shows that the value of $R_{\max}$ doesn't have considerable effects on these diagrams, because the variation of the flow temperature against r is highly affected by the velocity u and this velocity component doesn't change much with the dimension of the solution domain. According to Fig. 11, the value of the Nusselt number is constant along the cylinder's axis, as it is expected. Only near the boundaries we witness a slight variation in Nu which is due to our approximation for the boundary conditions (Eq. (10)). Ignoring this little error, we can express that for $Re = 1, 5, 10$, 15, 20 the average values of the Nusselt number are $0.73, 1.37, 1.85$, 2.21, 2.54, respectively. The peripheral shear-stress shown in Fig. 12 has similar situation too. It can clearly be seen from Fig. 13 that the axial shear-stress on the cylinder's surface has linear variation along the z-axis. Since $Gr = 0$, the flow is symmetric against the line $z = 0$ and so $(\tau_w)_z = 0$ (stagnation point) occurs exactly at $z = 0$, too (see Fig. 14).

The effect of the cylinder's rotating speed (parameter Ω. Re) on the value of the Nusselt number at $z = 0$ is shown in Fig. 13 for $Re = 1, 5, 10$. It seems in this figure that the Nusselt number has no variations against Ω but actually it has a slight reduction which is not clear because of the wide range used in vertical axis of the diagram. For this reason, we tabulated the numerical results in Table 2 to illustrate Nu variation more sensibly. According to these values, for example for $Re = 1$, when Ω. Re changes from 0 to 25, Nusselt number reduces from 0.73 to 0.722 (i.e. 1.1% reduction). Similarly, for $Re = 5, 10$ there are 0.39% and 0.13% reduction in Nu. Therefore, we can conclude that although velocity v can affect u and w according to Eq. (4) and they affect θ as in Eq. (7), but velocity v doesn't affect the temperature distribution and so the Nusselt

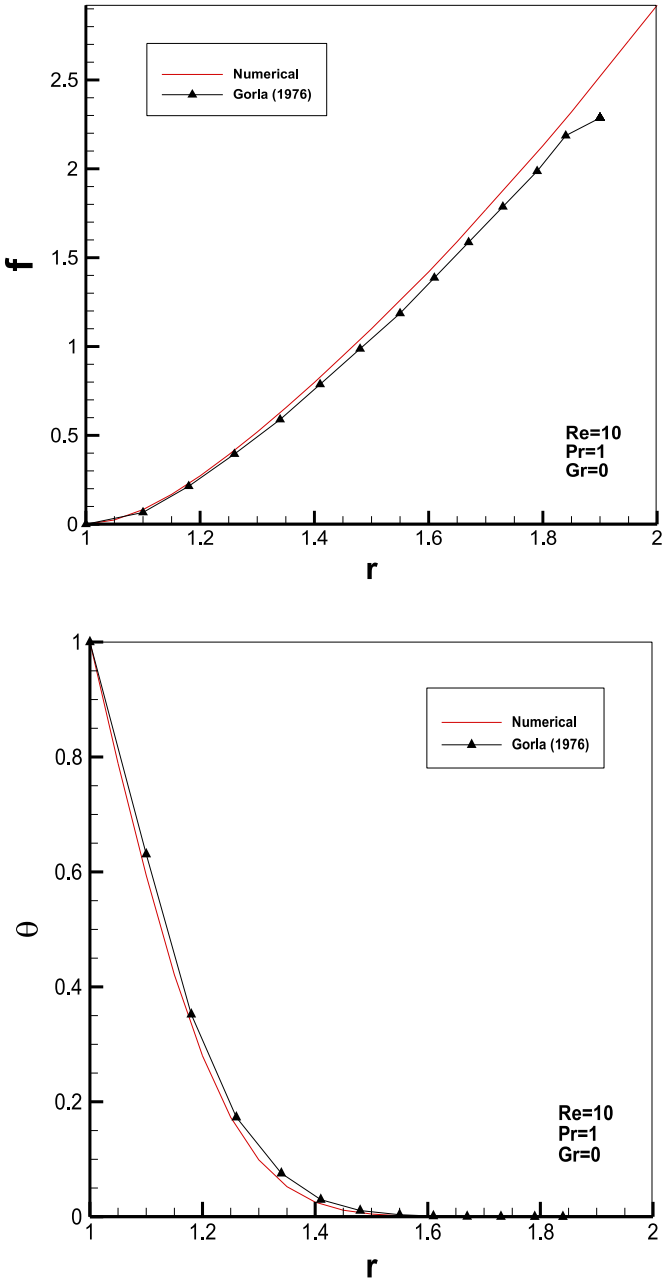

Fig. 7. Distribution of radial velocity function f and thermal function θ at $z = 1$ for $Re = 10$, Pr = 1, $Gr = 0$ and $R_{\max} = 2.8$, $z_{\min,\max} = \pm 4$.

number considerably. This result is a confirmation for the obtained conclusion in Ref. [21] regarding rotating horizontal cylinder via exact solution using similarity method. A linear relation between Ω and $(\tau_w)_\varphi$ is being demonstrated in Fig. 15 for selected values of Reynolds number. Also, it shows that higher Reynolds number causes a larger peripheral shear-stress at each specific cylinder's rotating speed. The relation between the position of the stagnation-point along z-axis z_s to the value of Grashof number for $Re = 1, 5, 10$ is depicted in Fig. 16. This is a linear relation if we use the parameter $Gr/Re2$ as the variable. It is noticeable that for a specific Re, when buoyancy forces (Grashof number) increase which is indication of dominance of free convection over forced convection, the stagnation-point moves downward along the cylinder's axis in opposite direction of the buoyancy forces. It means that the

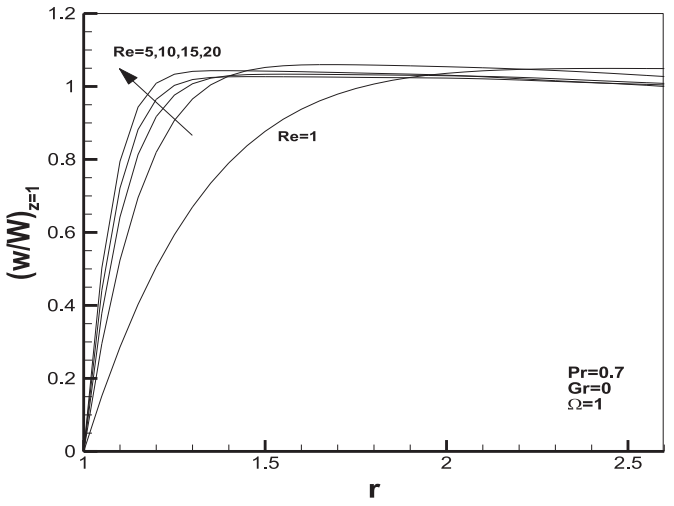

Fig. 8. Distribution of axial velocity *w (r, z)* against *r* for *Re = 1, 5, 10, 15, 20* with *pr* = 0.7, *Gr = 0* and *Ω = 1*.

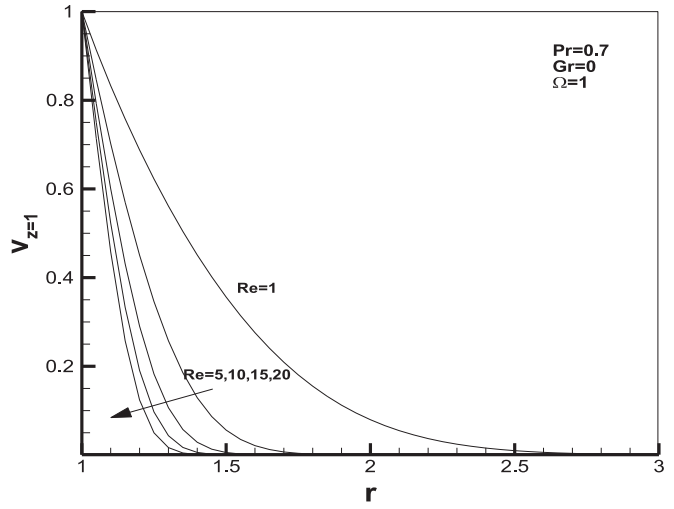

Fig. 9. Distribution of peripheral velocity *v* against *r* for *Re = 1, 5, 10, 15, 20* with *pr* = 0.7, *Gr = 0* and *Ω = 1*.

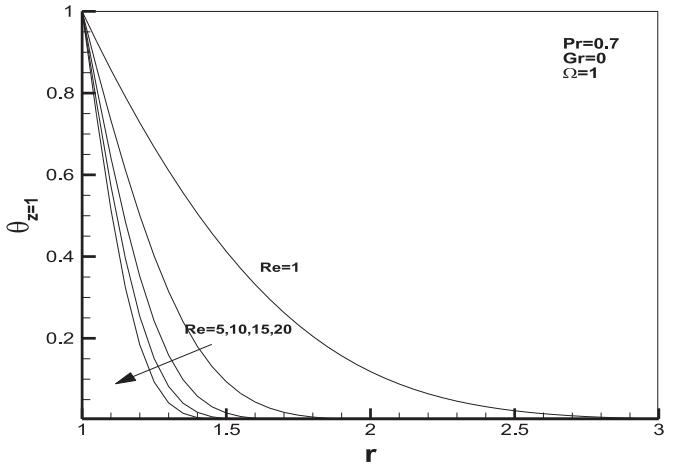

Fig. 10. Distribution of thermal function *θ (r, z)* against *r* for *Re = 1, 5, 10, 15, 20* with *pr* = 0.7, *Gr = 0* and *Ω = 1*.

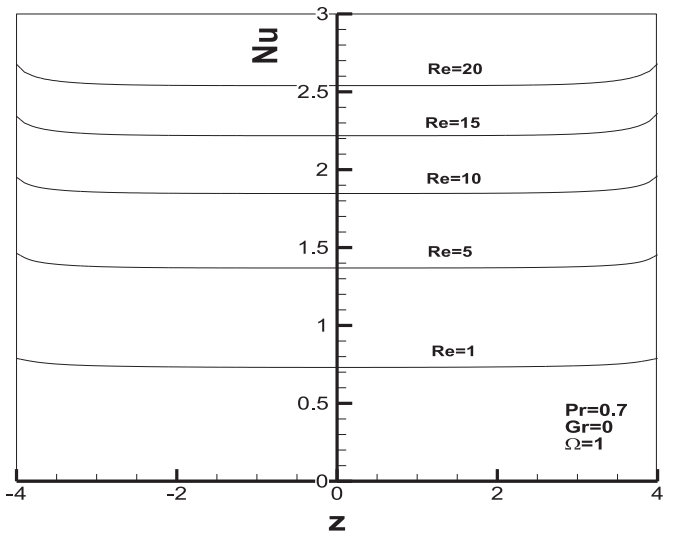

Fig. 11. Variation of Nusselt number against *z* for *Re = 1, 5, 10, 15, 20* with *pr* = 0.7, *Gr = 0* and *Ω = 1*.

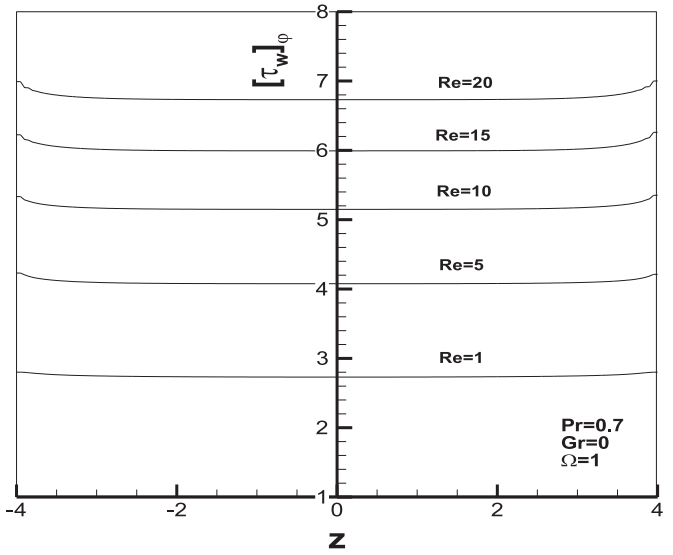

Fig. 12. Variation of peripheral wall shear-stress against *z* for *Re = 1, 5, 10, 15, 20* with *pr* = 0.7, *Gr = 0* and *Ω = 1*.

buoyancy forces don't move the stagnation-point directly, but they deform the flow streamlines in a way that the stagnation-point is located in the negative side of the *z*-axis. Besides, if the effective factor on the buoyancy forces (i.e. *Gr/Re2* according to Eq. (5)) is maintained constant, Reynolds number affects the value of z_s slightly.

We consider now the flow with constant parameters *Re = 1* and Pr = *0.7* but with variable Grashof numbers to show the effect of free convection dominance on the problem characteristics. Here we choose the dimensions of the domain of the solution as $R_{max} = 6$ and $z_{max,min} = \pm 4$, which are appropriate for *Re = 1*. The resulting diagrams are presented in Figs. 17–23 for *Gr = 0, 5, 10, 20, 50* and *100*. An assisting effect of the buoyancy forces in the distribution of velocity *w* in Fig. 17 is observed. This effect makes the velocity to grow, for example for *Gr = 50* up to *1.4* times more than the no-buoyancy condition. In the contrast, the opposing effect of the buoyancy forces which is shown in Fig. 18 at *z = -1*, can decrease

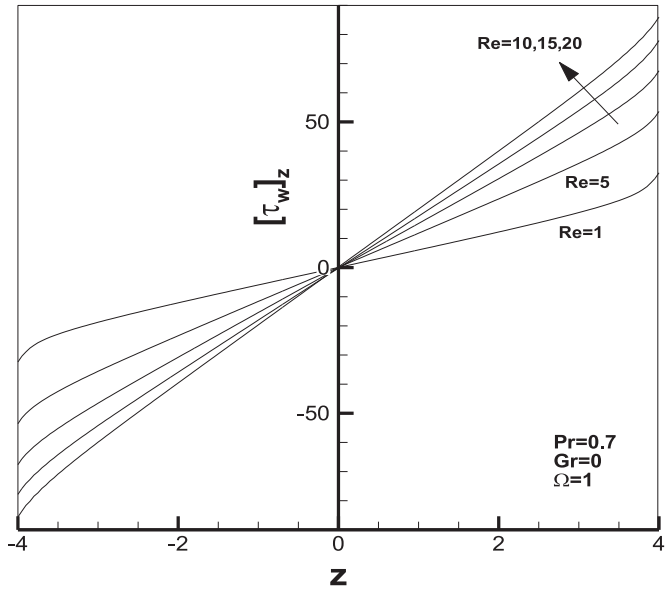

Fig. 13. Variation of axial wall shear-stress against z for $Re = 1, 5, 10, 15, 20$ with $pr = 0.7$, $Gr = 0$ and $\Omega = 1$.

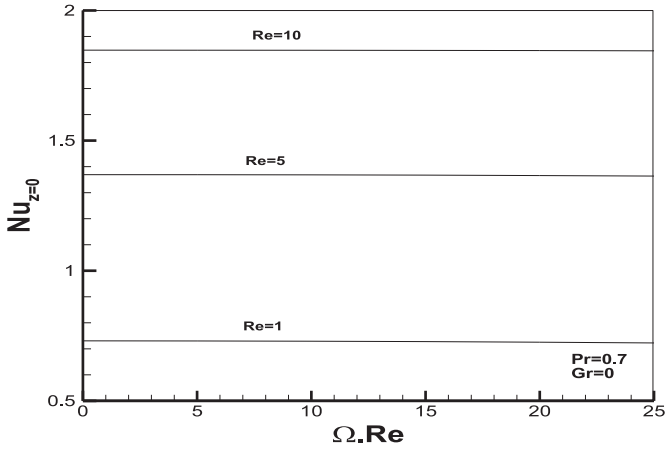

Fig. 14. Variation of Nusselt number at $z = 0$ against Ω. Re for $Re = 1, 5, 10$ with $pr = 0.7$ and $Gr = 0$.

Table 2
Numerical values of Nu at $z = 0$ against Ω.Re for $Re = 1, 5, 10$ with $pr = 0.7$ and $Gr = 0$ (used in Fig. 13).

Ω.Re	$Re = 1$	$Re = 5$	$Re = 10$
0	0.7305801	1.369128	1.847485
5	0.7302904	1.368865	1.847386
10	0.7293725	1.368278	1.847095
15	0.7278568	1.367415	1.846567
20	0.725469	1.365743	1.845967
25	0.7225865	1.363782	1.845069

velocity w to zero and even to reverse values (as it occurs for $Gr = 50$,100). According to Figs. 19 and 20, the distribution of the peripheral velocity v and the temperature θ shows very slight variations with various Grashof numbers. Similarly, the same issue exists for Nusselt number (Fig. 21). Therefore, at $z = 0$ we have Nusselt numbers *0.73, 0.73, 0.73, 0.722,* and *0.716* for $Gr = 0, 10, 20, 50$ and 100, respectively. In Fig. 22, which denotes the variations of

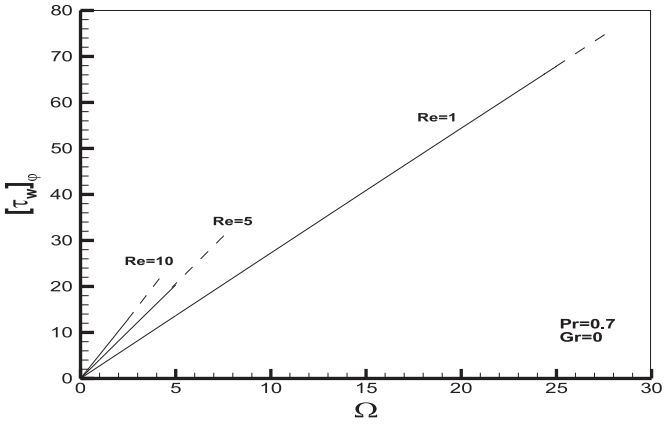

Fig. 15. Variation of peripheral wall shear stress at $z = 0$ against Ω for $Re = 1, 5, 10$ with $pr = 0.7$ and $Gr = 0$.

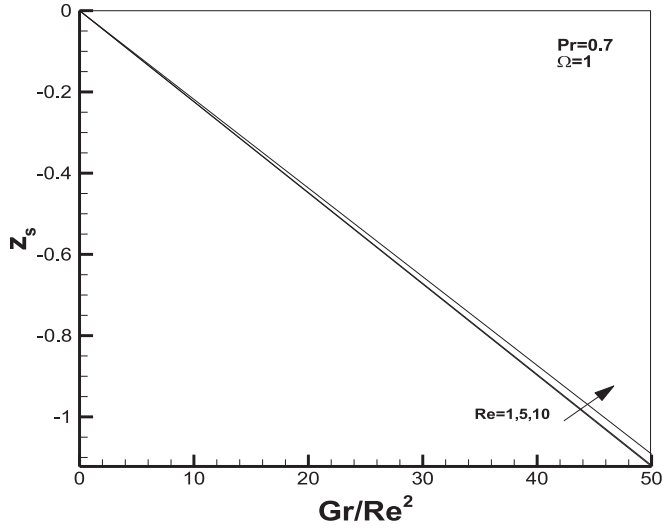

Fig. 16. Position of the stagnation point along z-axis against $Gr/Re2$for $Re = 1, 5, 10$ with $pr = 0.7$ and $\Omega = 1$.

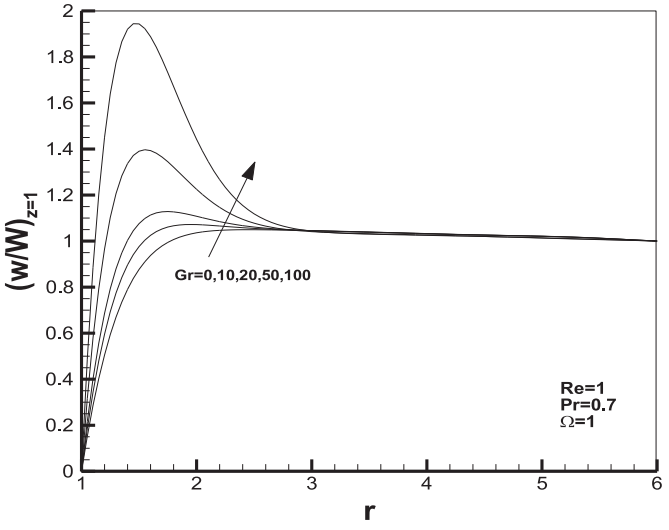

Fig. 17. Distribution of axial velocity $w\ (r, z = 1)$ against r for $Gr = 0, 10, 20, 50, 100$ with $Re = 1$, $pr = 0.7$ and $\Omega = 1$.

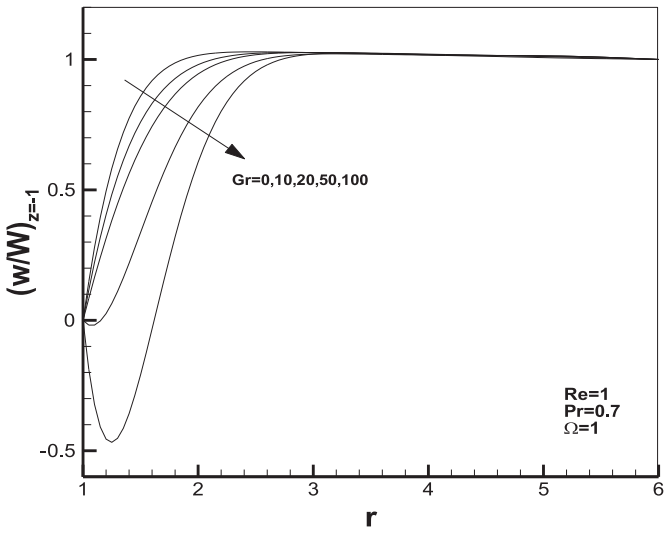

Fig. 18. Distribution of axial velocity $w\ (r, z = -1)$ against r for $Gr = 0, 10, 20, 50, 100$ with $Re = 1$, $pr = 0.7$ and $\Omega = 1$.

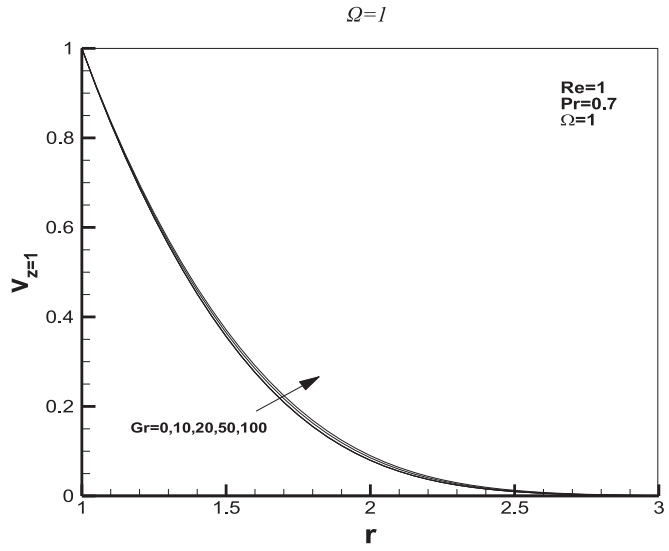

Fig. 19. Distribution of peripheral velocity $v\ (r, z = 1)$ against r for $Gr = 0, 10, 20, 50, 100$ with $Re = 1$, $pr = 0.7$ and $\Omega = 1$.

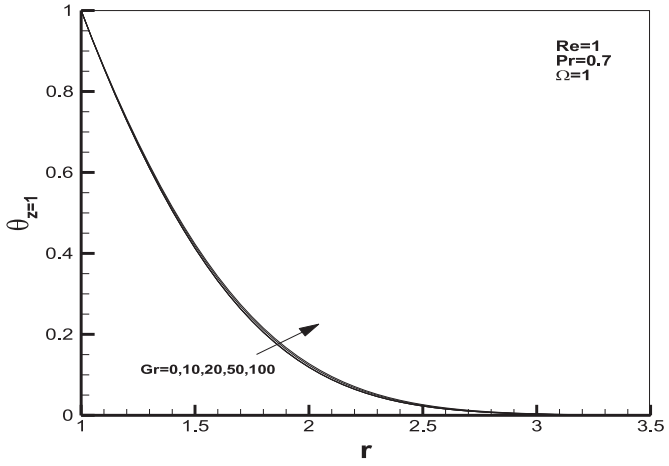

Fig. 20. Distribution of thermal function $\theta\ (r, z = 1)$ against r for $Gr = 0, 10, 20, 50, 100$ with $Re = 1$, $pr = 0.7$ and $\Omega = 1$.

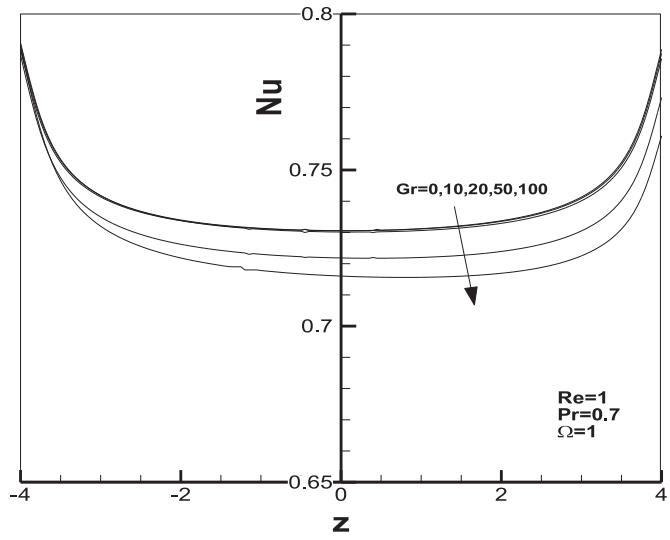

Fig. 21. Variation of Nusselt number against z for $Gr = 0, 10, 20, 50, 100$ with $Re = 1$, $pr = 0.7$ and $\Omega = 1$.

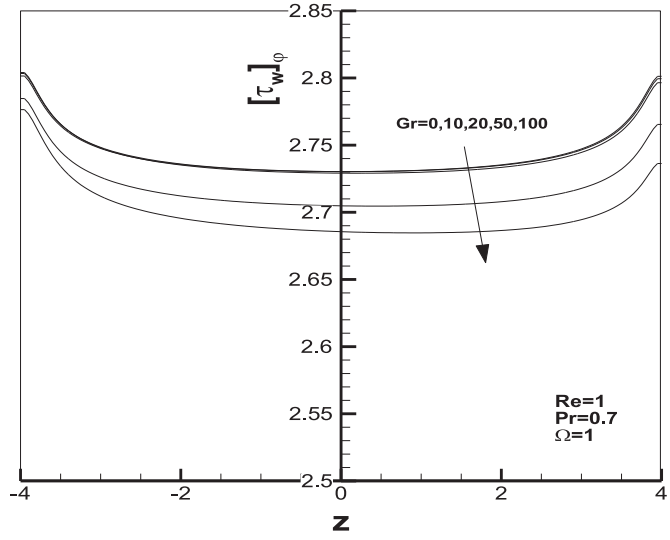

Fig. 22. Variation of peripheral wall shear-stress against z for $Gr = 0, 10, 20, 50, 100$ with $Re = 1$, $pr = 0.7$ and $\Omega = 1$.

peripheral shear-stress, we observe a trend similar to the variations of the Nusselt number. The central values of $(\tau_w)_\varphi$ for above mentioned Grashof numbers are *2.73, 2.73, 2.73, 2.7, and 2.68*, respectively. By referring to Fig. 23, it is understood that for larger Grashof numbers, which is the indication of dominance of the free convection over the forced convection, the shear-stress along the surface increases uniformly. The existence of the buoyancy forces moves the stagnation-point (the position of $\tau_w = 0$) downward. For instance, at $Gr = 20$, the stagnation-point is located at $z = -0.44$. Fig. 24 is an illustration of the flow stream-traces for two cases of $Gr = 0$ and $Gr = 50$. The effect of the buoyancy forces and consequently the stream-traces deformation near the wall are clearly visible for $Gr = 50$, as well as downward movement of the stagnation-point.

Finally, we illustrate the time-dependent variation of the two parameters $(\tau_w)_z$ and Nu in Figs. 25 and 26 for the case of $Re = 1$ and $\Omega = 1$, somewhere close to the stagnation-point ($z = 0.5$). As it can be seen, $(\tau_w)_z$ experiences an unstable variation along the time parameter τ, until it comes close to the steady-state condition. Also,

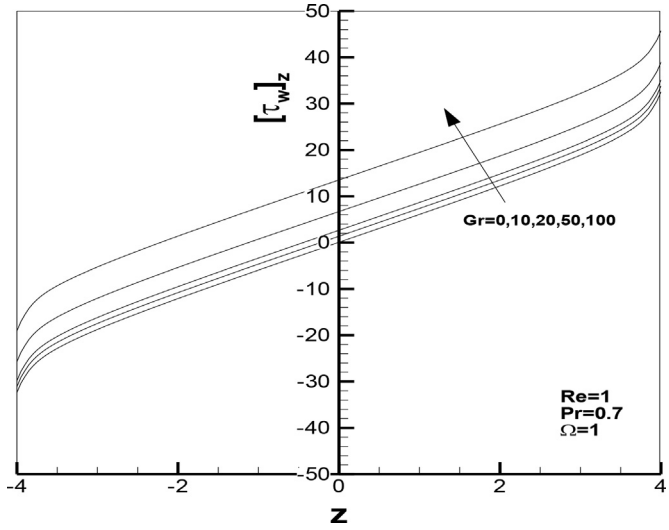

Fig. 23. Variation of axial wall shear-stress against z for $Gr = 0, 10, 20, 50, 100$ with $Re = 1$, $pr = 0.7$ and $\Omega = 1$.

a sudden change in the diagrams appears at about $\tau = 0.1$. Here is when the results of the numerical computation transfer from the initial inviscid values to the viscous results. After that, because of the gradual balancing of the pressure field over the computation domain, there is an instability in the results which disappears over the time. The variation of the Nusselt number were plotted for three sample Prandtl numbers *0.7,7,70*. At the beginning instants of time, Nusselt numbers are almost the same regardless to the value of Pr but as the time passes it drops rapidly. This sudden drop is more severe for smaller Prandtl numbers which finally leads to a smaller Nu number in the steady-state case. Therefore, in the case of steady-state we will have $Nu = 0.73, 1.57, 3.86$ for $\mathrm{Pr} = 0.7, 7, 70$, respectively. As we know, the smaller the Prandtl number the higher the thermal diffusivity which causes the conduction heat transfer mechanism to dominate comparing to convection heat transfer and hence smaller Nusselt number is produced.

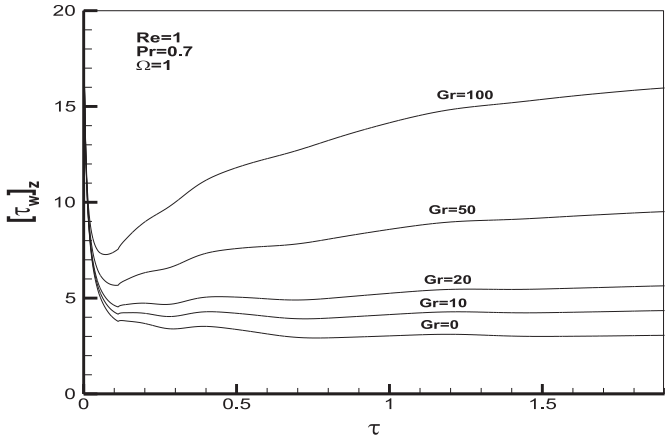

Fig. 25. Variation of axial wall shear-stress at $z = 0.5$ against time parameter τ for $Gr = 0, 10, 20, 50, 100$ with $Re = 1$, $pr = 0.7$ and $\Omega = 1$.

5. Conclusions

The unsteady problem of mixed convection heat transfer from a vertical cylinder impinged by an impulsive axisymmetric stagnation-point flow has been solved, numerically. A computational code, provided by the authors on the basis of SIMPLE algorithm, has been employed to predict the buoyancy effects and cylinder's rotating speed at different Reynolds numbers on the flow characteristics. For outer flow, which is supposed to be inviscid, simple analytical equations govern but in the domain of solution where flow has viscous behavior, Navier-Stokes and energy equations have been discretized and the resulting 4-equation system has been solved by an implicit finite-difference method. The steady-state result has been comparable to which formerly obtained by similarity solutions. The distribution of the velocity components u and w against r show that by choosing appropriate size of $R_{\max}$ for the domain of solution the numerical results of the problem would be close to the similarity ones. The importance of

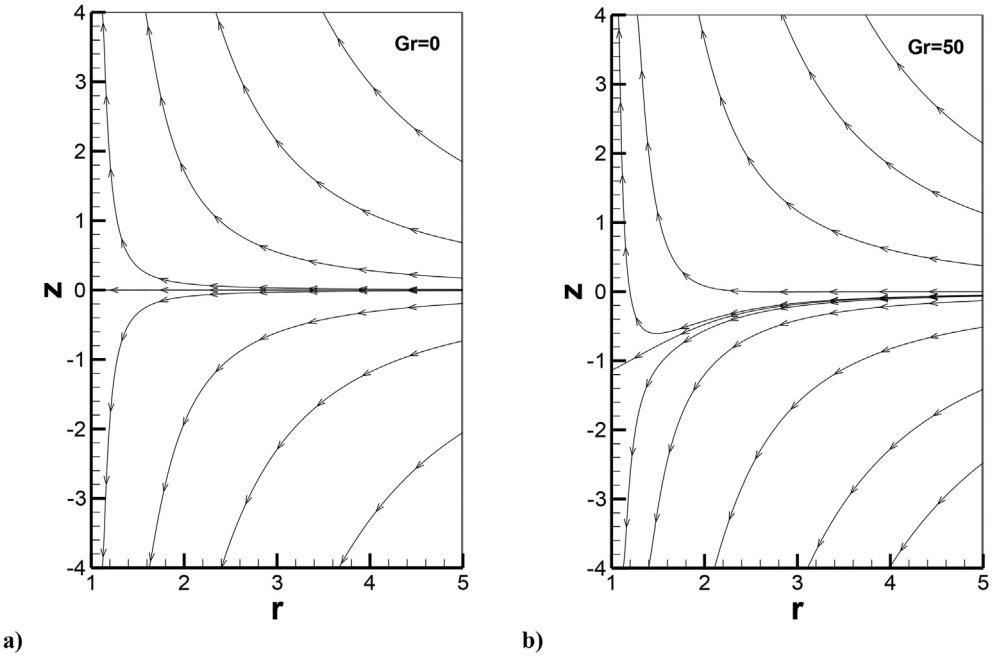

Fig. 24. Illustration of the flow Stream-traces for $Re = 1$, $pr = 0.7$, $\Omega = 0$: a) $Gr = 0$, b) $Gr = 50$.

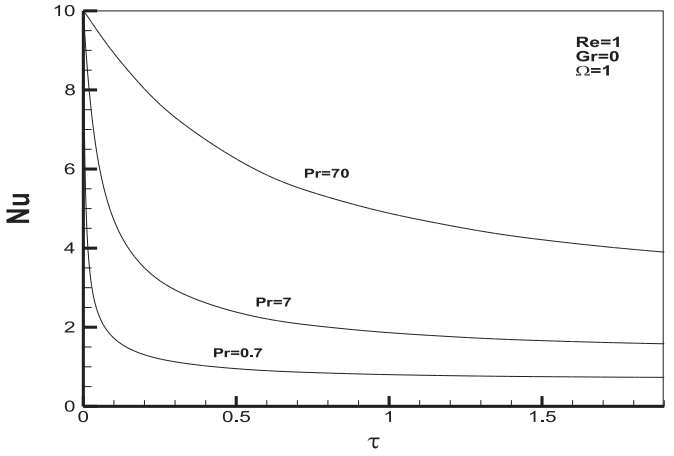

Fig. 26. Variation of Nusselt number at $z = 0.5$ against time parameter τ for $pr = 0.7, 7, 70$ with $Re = 1$, $Gr = 0$ and $\Omega = 1$.

the numerical method which has been presented here is due to the limitations of similarity method for solving all types of the problems. So, in the present paper after validation of the numerical method we have used it to solve the time-dependent problem at some different Reynolds and Grashof numbers. The results of the velocity and temperature has shown that in a specific condition the rotational speed of the cylinder can affect both the Nusselt number and the peripheral shear-stress on the cylinder's surface but very slightly. This confirms the results obtained for horizontal rotating cylinder in the literature using exact solution via similarity methods. Moreover, if the Grashof number gets to be a large value (depending on *Re*), the effect of buoyancy forces can completely deform the distribution of the velocity *w* and the flow streamtraces, as the stagnation-point locates itself below its normal position. Also, the Nusselt number and the peripheral shear-stress on the wall take a tiny reduction, when buoyancy forces exist. In other words, at high Grashof numbers, free convection heat transfer can affect the velocity field of the flow (components *u* and *w*) in a way that average values of *Nu* and $(\tau_w)_\varphi$ along the cylinder's axis partly decrease. It has also been shown that for a specific Reynolds number when buoyancy forces (Grashof number) increase which is indication of dominance of free convection over forced convection, the stagnation-point moves downward along the cylinder's axis in opposite direction of the buoyancy forces. Meaning that the buoyancy forces don't move the stagnation-point directly, but they deform the flow streamlines in a way that the stagnation-point is located in the negative side of the cylinder axis. Besides, if the effective factor on the buoyancy forces, *Gr/Re2*, is maintained constant, Reynolds number affects the value of the stagnation-point on the cylinder slightly.

Acknowledgment

This work has been financially supported by the office of research and development of Ferdowsi University of Mashhad under contract number 2/42668.

References

[1] Hiemenz K. Die Grenzchicht an einem in den gleichformingen Flussigkeitsstrom eingetauchten graden Kreiszylinder. Dinglers Polytech J 1911;236:321–410.
[2] Wang C. Axisymmetric stagnation flow on a cylinder. Q Appl Math 1974;10:207–13.
[3] Gorla RSR. Heat transfer in an axisymmetric stagnation flow on a cylinder. Appl Sci Res 1976;32(5):541–53.
[4] Gorla RSR. Unsteady laminar axisymmetric stagnation flow over a circular cylinder. Dev Mech 1977;9:286–8.
[5] Gorla RSR. Transient response behavior of an axisymmetric stagnation flow on a circular cylinder due to time dependent free stream velocity. Int J Eng Sci 1978;16(7):493–502.
[6] Gorla RSR. Viscous dissipation effects on heat transfer in an axisymmetric stagnation flow on a circular cylinder. Lett Heat Mass Transf 1978;5(2):121–30.
[7] Gorla RSR. Non-similar axisymmetric stagnation flow on a moving cylinder. Int J Eng Sci 1978;16(6):397–400.
[8] Gorla RSR. Unsteady viscous flow in the vicinity of an axisymmetric stagnation point on a circular cylinder. Int J Eng Sci 1979;17(1):87–93.
[9] Gorla RSR, Jankowski F, Textor D. Periodic boundary layer near an axisymmetric stagnation point on a circular cylinder. Int J Heat Fluid Flow 1988;9(4):421–6. http://dx.doi.org/10.1016/0142-727X(88)90010-0.
[10] Gorla RSR, Jankowski F, Textor D. Thermal response of a periodic boundary layer near an axisymmetric stagnation point on a circular cylinder. Int J Heat Fluid Flow 1988;9(4):427–30.
[11] Gorla RSR. Mixed convection in an axisymmetric stagnation flow on a vertical cylinder. Acta Mech 1993;99(1–4):113–23.
[12] Gorla RSR. Combined forced and free convection in an axisymmetric stagnation flow on a vertical non-isothermal cylinder. Wärme-und Stoffübertragung 1993;28(3):153–7.
[13] Cunning GM, Davis A, Weidman P. Radial stagnation flow on a rotating circular cylinder with uniform transpiration. J Eng Math 1998;33(2):113–28.
[14] Takhar H, Chamkha A, Nath G. Unsteady axisymmetric stagnation-point flow of a viscous fluid on a cylinder. Int J Eng Sci 1999;37(15):1943–57.
[15] Gorla RSR, Salem A, Mansour M, El-Hawary H. Chebyshev approximation for heat transfer in an axisymmetric stagnation flow on a cylinder. CHMT Digit Libr Online 2001;4.
[16] Rahimi AB. Heat transfer in an axisymmetric stagnation flow at high Reynolds numbers on a cylinder using perturbation techniques. Sci Iran 2003;10(1):116–21.
[17] Saleh R, Rahimi AB. Axisymmetric stagnation point flow of a viscous fluid on a moving cylinder with time dependent axial velocity. Int J Eng 2004;17(1):8.
[18] Saleh R, Rahimi AB. Axisymmetric stagnation-point flow and heat transfer of a viscous fluid on a moving cylinder with time-dependent axial velocity and uniform transpiration. J Fluids Eng 2004;126(6):997–1005.
[19] Rahimi AB. Stagnation flow and heat transfer on a moving cylinder with transpiration and high Reynolds numbers. Iran J Sci Technol -Trans B Eng 2004;28(B4):400–12.
[20] Saleh R, Rahimi AB. Stagnation flow and heat transfer on a moving cylinder with transpiration and high Reynolds numbers consideration. Iran J Sci Technol 2004;28(B4):453–66.
[21] Saleh R, Rahimi AB. Axisymmetric radial stagnation-point flow of a viscous fluid on a rotating cylinder with time-dependent angular velocity. Sci Iran 2005;12(4):329–37.
[22] Wang C. Stagnation flow on a cylinder with partial slip—an exact solution of the Navier–Stokes equations. IMA J Appl Math 2007;72(3):271–7.
[23] Rahimi AB, Saleh R. Axisymmetric stagnation—point flow and heat transfer of a viscous fluid on a rotating cylinder with time-dependent angular velocity and uniform transpiration. J Fluids Eng 2007;129(1):106–15.
[24] Rahimi AB, Saleh R. Unaxisymmetric heat transfer in the axisymmetric stagnation-point flow of a viscous fluid on a cylinder with simultaneous axial and rotational movement along with transpiration. Sci Iran 2008;15(3):366–77.
[25] Rahimi AB, Saleh R. Similarity solution of unaxisymmetric heat transfer in stagnation-point flow on a cylinder with simultaneous axial and rotational movements. J Heat Transf 2008;130(5):054502.
[26] Revnic C, Grosan T, Merkin J, Pop I. Mixed convection flow near an axisymmetric stagnation point on a vertical cylinder. J Eng Math 2009;64(1):1–13.
[27] Haghighi B, Rahimi AB. Effect of time-dependent transpiration on axisymmetric stagnation-point flow and heat transfer of a viscous fluid on a moving circular cylinder. Energy 2010;2(3):4.
[28] Lok YY, Merkin JH, Pop I. Mixed convection flow near the axisymmetric stagnation point on a stretching or shrinking cylinder. Int J Therm Sci 2012;59:186–94. http://dx.doi.org/10.1016/j.ijthermalsci.2012.04.008.
[29] Mohammadiun H, Rahimi AB. Stagnation-point flow and heat transfer of a viscous, compressible fluid on a cylinder. J Thermophys Heat Transf 2012;26(3):494–502.
[30] Mohammadiun H, Rahimi AB, Kianifar A. Axisymmetric stagnation-point flow and heat transfer of a viscous, compressible fluid on a cylinder with constant heat flux. Sci Iran 2013;20(1):185–94. http://dx.doi.org/10.1016/j.scient.2012.12.015.
[31] Najib N, Bachok N, Arifin N, Ishak AM. Boundary layer stagnation point flow and heat transfer past a permeable exponentially shrinking cylinder. Int J Math Model Methods Appl Sci 2014;8(1):121–6.
[32] N. Najib, N. Bachok, N.M. Arifin, "Stagnation point flow over a stretching/shrinking cylinder with prescribed surface heat flux", Paper presented at the Proceedings of the 3RD International Conference on Mathematical Sciences.
[33] Alizadeh R, Rahimi AB, Najafi M. Unaxisymmetric stagnation-point flow and heat transfer of a viscous fluid on a moving cylinder with time-dependent axial velocity. J Braz Soc Mech Sci Eng 2016;38(1):85–98.
[34] Rahimi AB, Mohammadiun H, Mohammadiun M. Axisymmetric stagnation flow and heat transfer of a compressible fluid impinging on a cylinder moving axially. J Heat Transf 2016;138(2):022201.